ISSN 0915-633X

NATIONAL INSTITUTE FOR FUSION SCIENCE

Basis Set Approach in the Constrained Interpolation Profile Method

T. Utsumi, J. Koga, T. Yabe, Y. Ogata, E. Matsunaga,
T. Aoki and M. Sekine

(Received - July 9, 2003)

NIFS-778 July 2003

TOKI, JAPAN

Basis set approach in the Constrained Interpolation Profile Method

T. Utsumi, and J. Koga
Advanced Photon Research Center, Japan Atomic Energy Research Institute, 8-1 Umemidai Kizu-cho, Souraku-gun, Kyoto 619-0215, Japan

T.Yabe, Y. Ogata, and E. Matsunaga
Department of Mechanical Engineering and Science, Tokyo Institute of Technology, O-okayama, Meguro-ku, Tokyo 152-8552, Japan

T. Aoki
Global Scientific Information and Computing Center, Tokyo Institute of Technology, O-okayama, Meguro-ku, Tokyo 152-8552, Japan

M. Sekine
Division of Electrical and Electronic Engineering, Tokyo University of Agriculture and Technology, 2-24-16 Nakamachi, Koganei, Tokyo, 184-8588, Japan

We propose a simple polynomial basis-set that is easily extendable to any desired higher-order accuracy. This method is based on the Constrained Interpolation Profile (CIP) method and the profile is chosen so that the subgrid scale solution approaches the real solution by the constraints from the spatial derivative of the original equation. Thus the solution even on the subgrid scale becomes consistent with the master equation. By increasing the order of the polynomial, this solution quickly converges. 3rd and 5th order polynomials are tested on the one-dimensional Schrödinger equation and are proved to give solutions a few orders of magnitude higher in accuracy than conventional methods for lower-lying eigenstates.

Keywords: CIP-BS method, CIP method, basis set, Schrödinger equation

PACS numbers: 02.60.Lj, 02.70.-c, 03.67.Lx

There is a growing interest in computational design of material properties, catalysis, medical drugs, and so on. For this purpose, we need accurate solutions of the excited states of atoms and their time dependent solutions. Much pioneering work have been performed with this goal in mind [1–4].

The purpose of this paper is to establish a systematic and simple method to get solutions with any desired accuracy by the use of the Constrained Interpolation Profile (CIP) method. The CIP method was first proposed by one of the authors for the solution of hyperbolic-type equations [5–8]. In its original form, it used a cubic polynomial to describe the subgrid-scale profile. All the coefficients of the polynomial are determined so that the piece-wise polynomial can reproduce a local analytical solution within a grid cell by the constraints from the spatial derivatives of the original equation. Resultingly, the CIP method can accurately describe the solution of a propagating wave having a wavelength of only two grid cells, which is beyond the capability of existing schemes. In this paper, we apply this method to the one-dimensional Schrödinger equation and obtain very accurate solutions which are a few orders of magnitude better than conventional methods for lower-lying eigenstates. It is important to note that the scheme is easily extended to higher order polynomials or to other functions with any desired accuracy by simply adopting the higher-order derivatives of the original equations as constraints to generate a self-consistent subgrid profile.

We need a basis set where it is easy to define values and derivatives of an arbitrary function $f(x)$ at the grid points. Therefore, we assume that the functions in the domain of R^1 can be approximated by the CIP-basis set of degree K method (CIP-BS^K), where K refers to the order of the derivatives we retain in the calculation, through the expression

$$f(x) = \sum_{i=1}^{N} \sum_{k=0}^{K} f_i^{(k)} \phi_{k,i}(x), \tag{1}$$

where $f_i^{(k)}$ is the k-th coefficient at the grid point x_i, the summation on the index i is taken over all grid points, and the basis functions $\phi_{k,i}(x)$ on the local support $[x_{i-1}, x_{i+1}]$ are expressed in the form

$$\begin{aligned} \phi_{k,i}(x) &= (\theta(x - x_{i-1}) - \theta(x - x_i))\phi_{k,i-}(x) \\ &+ (\theta(x - x_i) - \theta(x - x_{i+1}))\phi_{k,i+}(x), \end{aligned} \tag{2}$$

where $\theta(x)$ is the Heaviside step function, and $\phi_{k,i-}(x), \phi_{k,i+}(x)$ are polynomials of degree $(2K+1)$ determined from the constraints at the grid points

$$\begin{aligned} D_x^l \phi_{k,i-}(x_i) &= \begin{cases} 1 & for \quad l = k \\ 0 & for \quad l = 0, 1, \cdots, k-1, k+1, \cdots, K \end{cases} \\ D_x^l \phi_{k.i-}(x_{i-1}) &= 0 \quad for \quad k = 0, 1, \cdots, K, \end{aligned} \tag{3}$$

and

$$D_x^l \phi_{k,i+}(x_i) = \begin{cases} 1 & for \quad l = k \\ 0 & for \quad l = 0, 1, \cdots, k-1, k+1, \cdots, K \end{cases}$$

$$D_x^l \phi_{k,i+}(x_{i+1}) = 0 \quad for \quad k = 0, 1, \cdots, K, \tag{4}$$

respectively, where D_x is the derivative operator in x, and $D_x^0 = 1$.

From this definition, we can verify that the basis functions for the CIP-BS^0 method are

$$\phi_{0,i-}(x) = 1 + \overline{x}/\Delta x_{i-}, \phi_{0,i+}(x) = 1 - \overline{x}/\Delta x_{i+}, \tag{5}$$

for the CIP-BS^1 method are

$$\begin{aligned}
\phi_{0,i-}(x) &= 1 - 3\overline{x}^2/\Delta x_{i-}^2 - 2\overline{x}^3/\Delta x_{i-}^3, \\
\phi_{0,i+}(x) &= 1 - 3\overline{x}^2/\Delta x_{i+}^2 + 2\overline{x}^3/\Delta x_{i+}^3, \\
\phi_{1,i-}(x) &= \overline{x} + 2\overline{x}^2/\Delta x_{i-} + \overline{x}^3/\Delta x_{i-}^2, \\
\phi_{1,i+}(x) &= \overline{x} - 2\overline{x}^2/\Delta x_{i+} + \overline{x}^3/\Delta x_{i+}^2,
\end{aligned} \tag{6}$$

and for the CIP-BS^2 method are

$$\begin{aligned}
\phi_{0,i-}(x) &= 1 + 10\overline{x}^3/\Delta x_{i-}^3 + 15\overline{x}^4/\Delta x_{i-}^4 + 6\overline{x}^5/\Delta x_{i-}^5, \\
\phi_{0,i+}(x) &= 1 - 10\overline{x}^3/\Delta x_{i+}^3 + 15\overline{x}^4/\Delta x_{i+}^4 - 6\overline{x}^5/\Delta x_{i+}^5, \\
\phi_{1,i-}(x) &= \overline{x} - 6\overline{x}^3/\Delta x_{i-}^2 - 8\overline{x}^4/\Delta x_{i-}^3 - 3\overline{x}^5/\Delta x_{i-}^4, \\
\phi_{1,i+}(x) &= \overline{x} - 6\overline{x}^3/\Delta x_{i+}^2 + 8\overline{x}^4/\Delta x_{i+}^3 - 3\overline{x}^5/\Delta x_{i+}^4, \\
\phi_{2,i-}(x) &= \overline{x}^2/2 + 3\overline{x}^3/2\Delta x_{i-} \\
&\quad + 3\overline{x}^4/2\Delta x_{i-}^2 + \overline{x}^5/2\Delta x_{i-}^3, \\
\phi_{2,i+}(x) &= \overline{x}^2/2 - 3\overline{x}^3/2\Delta x_{i+} \\
&\quad + 3\overline{x}^4/2\Delta x_{i+}^2 - \overline{x}^5/2\Delta x_{i+}^3,
\end{aligned} \tag{7}$$

where $\overline{x} = x - x_i$, $\Delta x_{i-} = x_i - x_{i-1}$, and $\Delta x_{i+} = x_{i+1} - x_i$. In particular, for a uniform grid system ($\Delta x_{i-} = \Delta x_{i+} = \Delta x$) the basis function satisfies the translational relation $\phi_{k,i}(x) = \phi_{k,i-n}(x - x_n)$.

In each grid interval we can see that the function $f(x)$ is approximated by linear, cubic, and quintic polynomials for the CIP-BS^0,-BS^1,-BS^2 method, respectively. For example, the interpolating function in $[x_i, x_{i+1}]$ for the CIP-BS^1 method is written by the Hermite type interpolation as $f(x) = c_0 + c_1\overline{x} + c_2\overline{x}^2 + c_3\overline{x}^3$, where $c_0 = f_i$, $c_1 = f_i^{'}$, $c_2 = 3(f_{i+1} - f_i)/\Delta x^2 - (2f_i^{'} + f_{i+1}^{'})/\Delta x$, $c_3 = 2(f_i - f_{i+1})/\Delta x^3 + (f_i^{'} + f_{i+1}^{'})/\Delta x^2$, and $\Delta x = x_{i+1} - x_i$. The coefficients $c_0 c_1, c_2, c_3$ are the same with those determined with the constraints: $f(x_i) = f_i$, $f^{'}(x_i) = f_i^{'}$, $f(x_{i+1}) = f_{i+1}$, $f^{'}(x_{i+1}) = f_{i+1}^{'}$. This is rewritten in the form of Eq.(1) as $f(x) = f_i\phi_{0,i+} + f_i'\phi_{1,i+} + f_{i+1}\phi_{0,i+1-} + f_{i+1}'\phi_{1,i+1-}$ in the interval $[x_i, x_{i+1}]$. Via the same procedure, we can verify that the CIP-BS^2 method gives coefficients equivalent to the ones used in the Interpolation Differential Operator (IDO) method [9], which is one of the extensions of the CIP method. This means that the definition the CIP-BS method through Eq.(1) is equivalent to the CIP representation.

The first derivative of the basis function is expressed as

$$\begin{aligned}
D_x\phi_{k,i}(x) &= (\delta(x - x_{i-1}) - \delta(x - x_i))\phi_{k,i-}(x) \\
&+ (\delta(x - x_i) - \delta(x - x_{i+1}))\phi_{k,i+}(x) \\
&+ (\theta(x - x_{i-1}) - \theta(x - x_i))\phi_{k,i-}^{'}(x) \\
&+ (\theta(x - x_i) - \theta(x - x_{i+1}))\phi_{k,i+}^{'}(x) \\
&= (\theta(x - x_{i-1}) - \theta(x - x_i))\phi_{k,i-}^{'}(x) \\
&+ (\theta(x - x_i) - \theta(x - x_{i+1}))\phi_{k,i+}^{'}(x)
\end{aligned} \tag{8}$$

where $\delta(x)$ is the Dirac delta function. Here, we have used the fact $\phi_{k,i\pm}(x)\delta(x - x_{i\pm1}) = 0$ due to the relation $x\delta(x) = 0$, and $\phi_{k,i-}(x_i) = \phi_{k,i+}(x_i)$. Similarly, we can obtain the l-th order derivatives of $\phi_{k,i}(x)$ for $l \leq K + 1$ as

$$\begin{aligned}
D_x^l\phi_{k,i}(x) &= (\theta(x - x_{i-1}) - \theta(x - x_i))\phi_{k,i-}^{(l)}(x) \\
&+ (\theta(x - x_i) - \theta(x - x_{i+1}))\phi_{k,i+}^{(l)}(x).
\end{aligned} \tag{9}$$

Although the basis functions are constructed by using distribution functions, the functions represented in the CIP-BS^K method belong to the C^K class.

It is easily found that the k-th spatial derivative of $f(x)$ at the grid point x_i equals the coefficient $f_i^{(k)}$, *i.e.* $D_x^k f(x)|_{x=x_i} = \frac{\partial^k}{\partial x^k} f(x_i) = f_i^{(k)}$. If $f(x) = 0$ in Eq.(1), we can deduce that all the coefficients $f_i^{(k)}$ are zero, and that the basis functions are linearly independent. The function $f(x)$ can also be written on this basis set as $\mathbf{f} = (\mathbf{f_1}, \mathbf{f_2}, \cdots, \mathbf{f_N})$, where $\mathbf{f_i} = (f_i^{(0)}, f_i^{(1)}, \cdots, f_i^{(K)})$.

To better understand the procedure we use to solve the differential equation that will be given below, we review the process of the CIP method in comparison with the CIP-BS^1 method. If the equation to be solved has a form like $\partial f/\partial t = L[f]$, where L is the spatial operator. then the time evolution of f at the grid point is given by this equation. The CIP method uses the derivative of this equation, $\partial f'/\partial t = dL/dx$, to determine the time evolution of f' at the grid point. Thus the profile inside the grid cell is described by $f(x) = f_i\phi_{0,i+} + f_i'\phi_{1,i+} + f_{i+1}\phi_{0,i+1-} + f_{i+1}'\phi_{1,i+1-}$ by using 4 constraints f, f' at the neighboring two grid points. Instead of using such an equation at each local grid point, we here use the integrated equation over the grid cell. Therefore, integration of the equation multiplied by $\phi_{0,i}$ picks up the contribution from f and corresponds to $\partial f/\partial t = L[f]$ while the integration with $\phi_{1,i}$ corresponds to $\partial f'/\partial t = dL/dx$ as in the CIP method. The prediction of the value and derivative based on the original equation is thus realized by the following inner product.

$$< g|f > \equiv \int_R g(x)f(x)dx = (\mathbf{g}, S\mathbf{f}), \tag{10}$$

where S is a positive-definite matrix with the element $S_{k'i',ki} = < \phi_{k',i'}|\phi_{k,i} >$. Since $S_{k'i',ki}$ is non-zero only for $i = i^{'} - 1, i^{'}, i^{'} + 1$, S is a banded diagonal matrix with bandwidth $3(K + 1)$. The matrix representation of an analytic function $u(x)$ also has the same structure as the matrix S, and the matrix elements $< \phi_{k',i'}|u|\phi_{k,i} >$ can be analytically calculated. The matrix elements of the differential operator $< \phi_{k',i'}|D_x^l|\phi_{k,i} >$ can be defined properly for $l \leq K + 1$ with the use of Eq.(9), and by taking a partial integral the following relation holds

$$< \phi_{k',i'}|D_x^l|\phi_{k,i} > = (-1)^m < D_x^m\phi_{k',i'}|D_x^{l-m}|\phi_{k,i} >$$

$$for\ m\ =\ 0, 1, \cdots, l. \tag{11}$$

It is worth noting that we can extend the above definition to $l = K+2$. This can be seen by directly taking the $(K+2)$-th derivative of $\phi_{k,i}(x)$ and considering that $\phi_{k'i'}(x)$ is zero at $x = x_{i-1}, x_{i+1}$ and continuous at $x = x_i$. This means that even for $K = 0$, *i.e.* the CIP-BS^0 method, the matrix elements of second order derivatives are well defined. To clarify the role of the inner product, we list the following examples calculated in the CIP-BS^0 basis set.

$$\begin{aligned} < \phi_{0,i}|f(x) > &= (\frac{1}{6}f_{i-1} + \frac{2}{3}f_i + \frac{1}{6}f_{i+1})\Delta x \\ < \phi_{0,i}|D_x|f(x) > &= (-\frac{1}{2}f_{i-1} + \frac{1}{2}f_{i+1}) \\ < \phi_{0,i}|D_x^2|f(x) > &= (f_{i-1} - 2f_i + f_{i+1})/\Delta x \end{aligned} \tag{12}$$

These simple illustrations indicate that taking the inner products is a kind of procedure to extract approximated local properties of the function.

Writing the wave function as $\varphi(x,t) = \sum_{i=1}^{N}\sum_{k=0}^{K} a_i^{(k)}(t)\phi_{k,i}(x)$, where $a_i^{(k)}(t)$ is a complex number, the one-dimensional time dependent Schrödinger equation in an external potential $V(x,t)$

$$i\frac{\partial\varphi(x,t)}{\partial t} = -\frac{1}{2m}D_x^2\varphi(x,t) + V(r,t)\varphi(x,t) \tag{13}$$

is reduced to the ordinary differential equation

$$iS\frac{d}{dt}\mathbf{a}(t) = (H_0 + H_I(t))\mathbf{a}(t), \tag{14}$$

where atomic units ($\hbar = e = m_e = 1$) are used, and the matrix S, H_0, and $H_I(t)$ are banded diagonal matrices with bandwidth $3(K+1)$. The matrix elements of H_0 and $H_I(t)$ are $-\frac{1}{2m} < \phi_{k',i'}|D_x^2|\phi_{k,i} >$ and $< \phi_{k',i'}|V(x,t)|\phi_{k,i} >$, respectively. In general, this procedure is used to form equations for the coefficients $f_i^{(k)}$ from the the ordinary and partial differential equations for $f(x)$. Even if nonlinear terms are involved, for example $H_I = c\varphi(x,t)^2$, the structure of the matrices is same as one for the linear equation except that the coefficients $f_i^{(k)}$ would be included.

In the case of the stationary potential, the energy spectrum is obtained by setting $a_i^{(k)}(t) = \exp(-i\lambda t)a_i^{(k)}$ and solving the generalized eigenvalue equation

$$(H_0 + H_I)\mathbf{a} = \lambda S\mathbf{a}. \tag{15}$$

We have applied the proposed idea to the Schrödinger equation to demonstrate it's efficiency and accuracy. For simplicity we consider the one-dimensional eigenvalue problem Eq.(15) with a uniform grid. The extension to multidimensional problems or non-uniform grid systems is straightforward in a manner similar to the CIP method [7]. Furthermore, it is easy to solve the time-dependent Schrödinger equation Eq.(14) by means of either an explicit or implicit time propagation scheme [10].

For the first case, we consider eigenvalue spectrum for the Schrödinger equation for the free electron in a box. The results are shown in Tables I and II, where the box size is taken to be 1.0 a.u and the number of grids N is 50. As seen from the error, the results by the CIP-BS^2 method, which includes second derivatives, are 10^5 to 10^6 times more accurate than those by the CIP-BS^1 method. The zero derivative boundary condition at grid point N is built in by setting $a_N^1 = 0$ (*i.e.*, $\varphi'(r_N) = 0$). In the same way setting the boundary to zero is done by setting $a_N^0 = 0$ (*i.e.*, $\varphi(0) = 0$). Since the derivatives are included in the state vector $\mathbf{a}$, incorporation of the boundary conditions can be achieved keeping a one-to-one correspondence to the analytical ones. Periodic or other types of boundary conditions can also be treated in the same manner. Although we use basis functions that do not satisfy boundary conditions, it is not necessary to add a Bloch operator to the Hamiltonian like the discrete variable representation (DVR) method [3]. The numerical results in Tables I and II indicate good agreement with the exact values.

For the second case, we consider the eigenvalue spectrum for the radial Schrödinger equation of the hydrogen atom. The system size is set to 1000.0 a.u. in order to obtain sufficient precision for states with a high principal quantum number n. In Table III we present the results of energy levels for $s-$, $p-$, and $d-$orbitals. Here the grid interval is 1.0 a.u. and the boundary condition $\varphi(0) = \varphi(r_N) = 0$ is imposed for this eigenvalue problem. We can see that the eigenvectors simultaneously contain derivatives consistent with the eigenfunctions from samples of the calculated orbitals shown in Figure 1. The results show excellent agreement with the analytical spectrum. It should be emphasized that the singularities due to the kinetic operator $(\frac{1}{r^2})$ and the Coulomb potential $(\frac{1}{r})$ at $r = 0$ are eliminated in the Hamiltonian by taking the inner product.

For the third case, we consider the eigenvalue spectrum for the Schrödinger equation in the Morse potential, $V(x) = D[(e^{-2\alpha x} - 2e^{-\alpha x}) + 1]$, which excellently describes the vibrations of a two-atom molecule. Using the variable $z = \frac{2\gamma}{\alpha}e^{-\alpha x}$, where $\gamma = (2mD)^{1/2}$, the equation turns out to be a confluent hypergeometric equation so that the complete solution becomes [11]

$$\varphi(z) = z^{\beta/\alpha}e^{-z/2}\{C_1M(a,b,z) + C_2U(a,b,z)\}, \tag{16}$$

where $\beta = (2m(D-E))^{1/2}$, $c = \frac{2\beta}{\alpha} + 1$, $a = \frac{c}{2} - \frac{\gamma}{\alpha}$, $M(a,b,z)$ and $U(a,b,z)$ are Kummer's functions, m is the reduced mass, and E is the energy of the system. For the bound state, the constant C_2 must vanish, the constant C_1 is fixed by the normalization, and the eigenenergy must be determined from the relation $a = -n$, where n is a non-negative integer which satisfies $0 < E < D$. The results are shown in Table IV, where the parameters are $\alpha = 0.9374$ a.u., $D = 0.0224$ a.u., $m = 119406$ a.u., and $-0.8 \leq x \leq 2.0$ (the interval of the system). These parameters are chosen to compare our results with those by Braun *et al.* [1] who used the block-Lanczos

method with the Chebyshev approximation and Wei *et al.* [2] who used Lagrange Distributed Approximating Functionals (LDAFs). The boundary condition for the wave function is zero at $r = -0.8$ and $r = 2.0$ a.u. Our results are better than those of Braun *et al.* or Wei *et al.* for the lower-lying eigenstates. The high eigenvalues can be improved by enlarging the system size, and/or increasing the density of grid points. Although these dispositions induce the increase of the number of states, the computational time does not increase so rapidly due to the inherent locality of the CIP-BS method (narrower bandwidth).

While the CIP method has provided accurate solutions for various differential equations, especially for hydrodynamics, the CIP-BS method is more attractive for the analysis of quantum mechanical processes. The CIP-BS method, which is the reconstruction of the CIP method from the view point of the basis function of the Hermite type interpolating functions, has taken over the two important properties in the CIP method: (i) Any variable inside the grid cell is approximated not only by values but also the derivatives consistent with the governing equations. (ii) Interpolating functions are uniquely determined without problem- or algorithm-specific parameters. The system size and grid intervals are essentially inevitable parameters to be adjusted. The CIP-BS method offers additional advantages as follows: (i) It leads to banded diagonal matrices, which are easily adapted to a number of numerical methods developed for large, sparse linear systems [10], by transforming ordinary and partial differential equations. If the system is linear and contains only time-independent interactions, all the relevant matrices are constant and the time propagation of the wave function is carried out in a computationally efficient way. (ii) The boundary conditions are imposed with a one-to-one correspondence to the analytical ones. (iii) It provides a proper mean to relieve numerical difficulties due to singularities, *e.g.* Coulomb potential. (iv) Although our basis set is non-orthogonal, it introduces a close resemblance between quantum mechanics and numerical simulations.

Acknowledgment

This work was carried out under the collaborating research program at the National Institute for Fusion Science of Japan.

[1] M. Braun, S.A. Sofiaonos, D.G. Papageorgiou, and I.E. Lagaris, *J. Comput. Phys.* **126**, 315 (1996).
[2] G.W. Wei, D.S. Zhang, D.J. Kouri, and D.K. Hoffman, *Phys. Rev. Lett.* **79**, 775 (1997).
[3] B.I. Schneider, *Phys. Rev.* **A55**, 3417 (1997).
[4] C.J. Trahan, and R.E. Wyatt, *J. Comput. Phys.* **185**, 27 (2003).
[5] H. Takewaki, A. Nishiguchi, and T. Yabe, *J. Comput. Phys.* **61**, 261 (1985).
[6] T. Yabe and T. Aoki, *Comput. Phys. Commun.* **66**, 219 (1991).
[7] T. Yabe, T. Ishikawa, and P.Y. Wang, *Comput. Phys. Commun.* **66**, 233 (1991).
[8] T. Yabe, F. Xiao and T. Utsumi, *J. Comput. Phys.* **169**, 556 (2001).
[9] T. Aoki, *Comput. Phys. Commun.* **102**, 132 (1997).
[10] W.H. Press *et. al.*, *Numerical Recipes in Fortran 77*, (Cambridge Univ. Press, 1986).
[11] Siegfried Flügge, *Practical Quantum Mechanics*, (Springer-Verlag, New York, 1971)

TABLE I: Relative errors of eigenvalues of the free electron. The box size=1.0 a.u. and $N = 50$. The boundary condition for the wave function is zero at $r = 0$ a.u., and zero derivative at $r = 1.0$ a.u.

no.	Analytical	CIP-BS[1]	CIP-BS[2]
1	1.2337005501	$8.54\ 10^{-13}$	$6.75\ 10^{-13}$
2	11.103304951	$2.31\ 10^{-11}$	$1.23\ 10^{-13}$
3	30.842513753	$4.92\ 10^{-10}$	$4.07\ 10^{-14}$
4	60.451326957	$3.68\ 10^{-9}$	$1.12\ 10^{-14}$
5	99.929744561	$1.64\ 10^{-8}$	$2.70\ 10^{-14}$
6	149.27776657	$5.40\ 10^{-8}$	$9.65\ 10^{-14}$
7	208.49539297	$1.45\ 10^{-7}$	$1.01\ 10^{-13}$
8	277.58262378	$3.35\ 10^{-7}$	$1.34\ 10^{-13}$
9	356.53945899	$6.96\ 10^{-7}$	$4.38\ 10^{-13}$
10	445.36589860	$1.33\ 10^{-6}$	$1.33\ 10^{-12}$
11	544.06194261	$2.36\ 10^{-6}$	$3.68\ 10^{-12}$
12	652.62759102	$3.96\ 10^{-6}$	$9.39\ 10^{-12}$
13	771.06284384	$6.35\ 10^{-6}$	$2.22\ 10^{-11}$
14	899.36770105	$9.78\ 10^{-6}$	$4.93\ 10^{-11}$
15	103.75421627	$1.45\ 10^{-5}$	$1.04\ 10^{-10}$

TABLE II: Same as Table I. The boundary condition for the wave function is zero at $r = 1.0$ a.u.

no.	Analytical	CIP-BS[1]	CIP-BS[2]
1	4.9348022005	$2.83\ 10^{-12}$	$1.47\ 10^{-13}$
2	19.739208802	$1.30\ 10^{-10}$	$1.04\ 10^{-13}$
3	44.413219805	$1.46\ 10^{-9}$	$2.35\ 10^{-13}$
4	78.956835209	$8.15\ 10^{-9}$	$3.26\ 10^{-14}$
5	123.37005501	$3.07\ 10^{-8}$	$2.53\ 10^{-14}$
6	177.65287922	$9.03\ 10^{-8}$	$2.26\ 10^{-14}$
7	241.80530783	$2.24\ 10^{-7}$	$7.60\ 10^{-14}$
8	315.82734083	$4.89\ 10^{-7}$	$2.52\ 10^{-13}$
9	399.71897824	$9.70\ 10^{-7}$	$8.19\ 10^{-13}$
10	493.48022005	$1.78\ 10^{-6}$	$2.31\ 10^{-12}$
11	597.11106627	$3.08\ 10^{-6}$	$6.00\ 10^{-12}$
12	710.61151688	$5.04\ 10^{-6}$	$1.46\ 10^{-11}$
13	833.98157189	$7.92\ 10^{-6}$	$3.33\ 10^{-11}$
14	967.22123131	$1.20\ 10^{-5}$	$7.17\ 10^{-11}$
15	111.03304951	$1.75\ 10^{-5}$	$1.47\ 10^{-10}$

TABLE III: Relative errors of energy levels of bound states of the hydrogen atom with the CIP-BS^2 method. The system size is 1000.0 a.u. and the grid interval is 1.0 a.u. The boundary condition for the wave function is zero at $r = 0$ and $r = 1000.0$ a.u.

n	Analytical	$l = 0$	$l = 1$	$l = 2$
1	$-5.0000000000\ 10^{-1}$	$8.21\ 10^{-9}$		
2	$-1.2500000000\ 10^{-1}$	$2.77\ 10^{-10}$	$8.16\ 10^{-11}$	
3	$-5.5555555556\ 10^{-2}$	$7.34\ 10^{-11}$	$3.10\ 10^{-11}$	$1.40\ 10^{-12}$
4	$-3.1250000000\ 10^{-2}$	$3.88\ 10^{-11}$	$1.48\ 10^{-11}$	$3.63\ 10^{-13}$
5	$-2.0000000000\ 10^{-2}$	$2.37\ 10^{-11}$	$3.12\ 10^{-11}$	$6.25\ 10^{-12}$
6	$-1.3888888889\ 10^{-2}$	$2.76\ 10^{-11}$	$3.93\ 10^{-12}$	$1.12\ 10^{-11}$
7	$-1.0204081633\ 10^{-2}$	$2.40\ 10^{-11}$	$1.56\ 10^{-12}$	$1.31\ 10^{-12}$
8	$-7.8125000000\ 10^{-3}$	$4.09\ 10^{-12}$	$2.84\ 10^{-12}$	$1.32\ 10^{-12}$
9	$-6.1728395062\ 10^{-3}$	$3.10\ 10^{-12}$	$3.19\ 10^{-11}$	$5.93\ 10^{-12}$
10	$-5.0000000000\ 10^{-3}$	$2.17\ 10^{-12}$	$3.14\ 10^{-12}$	$7.90\ 10^{-12}$
11	$-4.1322314050\ 10^{-3}$	$3.92\ 10^{-12}$	$6.96\ 10^{-12}$	$6.73\ 10^{-12}$
12	$-3.4722222222\ 10^{-3}$	$3.56\ 10^{-12}$	$2.01\ 10^{-13}$	$8.85\ 10^{-12}$
13	$-2.9585798817\ 10^{-3}$	$3.94\ 10^{-12}$	$2.62\ 10^{-11}$	$5.75\ 10^{-12}$
14	$-2.5510204082\ 10^{-3}$	$4.23\ 10^{-12}$	$2.48\ 10^{-11}$	$4.37\ 10^{-12}$
15	$-2.2222222222\ 10^{-3}$	$1.11\ 10^{-11}$	$1.49\ 10^{-11}$	$5.34\ 10^{-12}$
16	$-1.9531250000\ 10^{-3}$	$9.86\ 10^{-12}$	$1.09\ 10^{-11}$	$1.71\ 10^{-12}$
17	$-1.7301038062\ 10^{-3}$	$7.61\ 10^{-12}$	$2.53\ 10^{-12}$	$3.48\ 10^{-12}$

TABLE IV: Relative errors of energy levels of bound states in the Morse potential with the CIP-BS^2 method for different grid numbers N. The boundary condition for the wave function is zero at $r = -0.8$ and $r = 2.0$ a.u. a) Braun *et al.*(Ref.[1],$N = 128$), b) Wei *et al.*(Ref.[2],$N = 100$)

no.	Analytical	$N = 70$	$N = 140$	Braun *et al.*[a]	Wei *et al.*[b]
1	$2.8617197881\ 10^{-4}$	$5.93\ 10^{-13}$	$1.73\ 10^{-13}$		
2	$8.5299662358\ 10^{-4}$	$2.91\ 10^{-12}$	$4.56\ 10^{-14}$	$1.18\ 10^{-8}$	$1.64\ 10^{-11}$
3	$1.4124621846\ 10^{-3}$	$1.12\ 10^{-11}$	$2.09\ 10^{-14}$	$2.13\ 10^{-8}$	$3.05\ 10^{-11}$
4	$1.9645686617\ 10^{-3}$	$3.49\ 10^{-11}$	$6.20\ 10^{-14}$	$2.55\ 10^{-8}$	$3.57\ 10^{-11}$
5	$2.5093160551\ 10^{-3}$	$9.15\ 10^{-11}$	$5.93\ 10^{-14}$	$2.80\ 10^{-8}$	$3.92\ 10^{-11}$
6	$3.0467043647\ 10^{-3}$	$2.09\ 10^{-10}$	$1.71\ 10^{-13}$	$2.90\ 10^{-8}$	$4.28\ 10^{-11}$
7	$3.5767335905\ 10^{-3}$	$4.31\ 10^{-10}$	$3.08\ 10^{-13}$	$3.08\ 10^{-8}$	$4.20\ 10^{-11}$
8	$4.0994037325\ 10^{-3}$	$8.15\ 10^{-10}$	$5.79\ 10^{-13}$		
9	$4.6147147907\ 10^{-3}$	$1.44\ 10^{-9}$	$9.88\ 10^{-13}$		
10	$5.1226667650\ 10^{-3}$	$2.39\ 10^{-9}$	$1.61\ 10^{-12}$		
11	$5.6232596556\ 10^{-3}$	$3.79\ 10^{-9}$	$2.49\ 10^{-12}$		
12	$6.1164934624\ 10^{-3}$	$5.77\ 10^{-9}$	$3.71\ 10^{-12}$	$3.27\ 10^{-8}$	$4.58\ 10^{-11}$
13	$6.6023681854\ 10^{-3}$	$8.48\ 10^{-9}$	$5.34\ 10^{-12}$		
14	$7.0808838246\ 10^{-3}$	$1.21\ 10^{-8}$	$7.47\ 10^{-12}$		
15	$7.5520403800\ 10^{-3}$	$1.68\ 10^{-8}$	$1.02\ 10^{-11}$		
16	$8.0158378516\ 10^{-3}$	$2.28\ 10^{-8}$	$1.37\ 10^{-11}$		
17	$8.4722762394\ 10^{-3}$	$3.02\ 10^{-8}$	$1.81\ 10^{-11}$	$3.31\ 10^{-8}$	$4.77\ 10^{-11}$
21	$1.0224438953\ 10^{-3}$	$7.91\ 10^{-8}$	$4.45\ 10^{-11}$	$3.39\ 10^{-8}$	$2.83\ 10^{-11}$

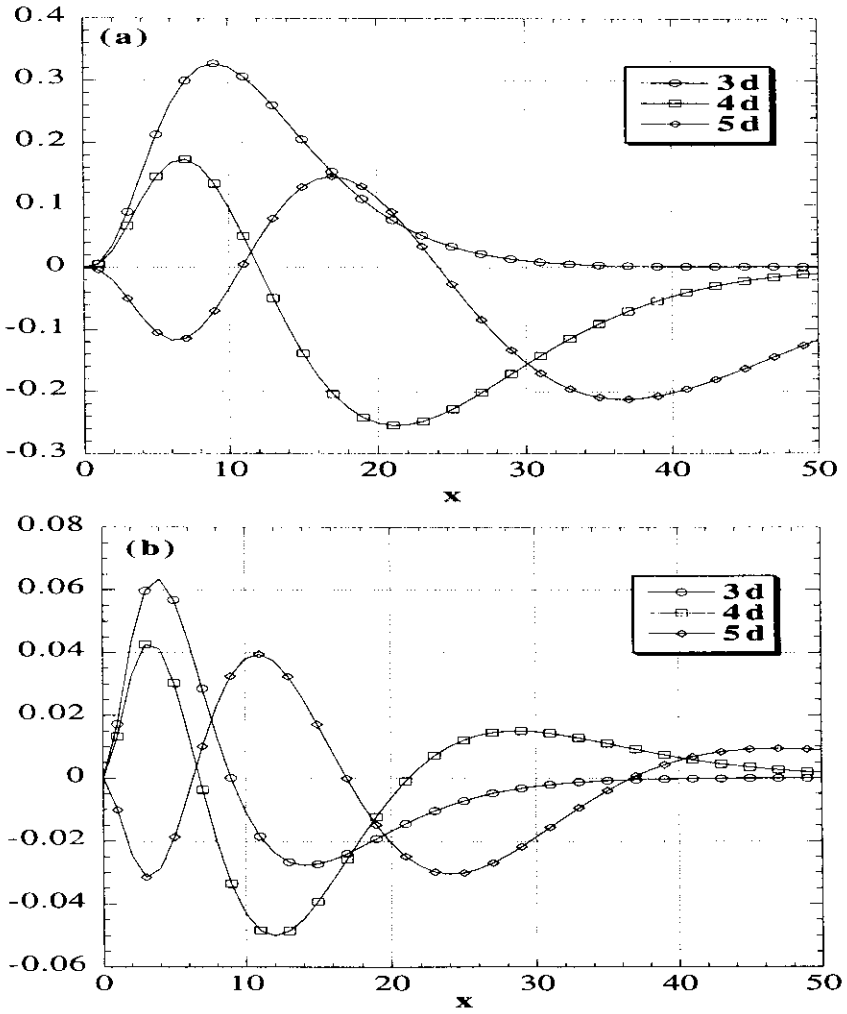

FIG. 1: The calculated (a) eigen functions and (b) their first derivatives for the $3d, 4d, 5d$ orbitals of the hydrogen atom. They are not normalized or interpolated.

Recent Issues of NIFS Series

NIFS-758 K. Toi, S. Ohdachi, S. Yamamotoa, N. Nakajima, S. Sakakibara, K.Y. Watanabe, S. Inagaki, Y. Nagayama, Y. Narushima, H. Yamada, K. Narihara, S. Morita, T. Akiyamab, N. Ashikawa, X. Dingc, M. Emoto, H. Funaba, M. Goto, K. Ida, H. Idei, T. Ido, K. Ikeda, S. Imagawa, M. Isobe, K. Itoh, O. Kaneko, K. Kawahata, T. Kobuchi, A. Komori, S. Kubo, R. Kumazawa, J. Lid, Y. Liang, S. Masuzaki, T. Mito, J. Miyazawa, T. Morisaki, S. Murakami, S. Muto, T. Mutoh, K. Nagaoka, Y. Nakamura, H. Nakanishi, K. Nishimura, A. Nishizawa, N. Noda, T. Notakea, K. Ohkubo, I. Ohtake, N. Ohyabu, Y. Oka, S. Okamura, T. Ozaki, B.J. Peterson, A. Sagara, T. Saidae, K. Saito, R. Sakamoto, M. Sasao, K. Sato, M. Sato, T. Satow, T. Seki, T. Shimozuma, M. Shoji, S. Sudo, M.Y. Tanaka, N. Tamurae, K. Tanaka, K. Tsumori, T. Uda, T. Watari, A. Wellerf, Y. Xu, I. Yamada, M. Yokoyama, S. Yoshimura, Y. Yoshimura, K. Yamazaki, K. Matsuoka, O. Motojima, Y. Hamada, M. Fujiwara
MHD Instabilities and Their Effects on Plasma Confinement in the Large Helical Device Plasmas
Oct. 2002 (EX/S3-2)

NIFS-759 S. Kubo, T. Shimozuma, H. Idei, Y. Yoshimura, T. Notake, M. Sato, K. Ohkubo, T. Watari,K. Narihara, I. Yamada, S. Inagaki, Y. Nagayama, S. Murakami, S. Muto,Y. Takeiri, M. Yokoyama, N. Ohyabu, K. Ida, K. Kawahata, O. Kaneko, A. Komori, T. Mutoh, Y. Nakamura, H. Yamada, T. Akiyama, N. Ashikawa, M. Emoto, H. Funaba, P. Goncharov M. Goto, K. Ikeda, M. Isobe, H. Kawazome, K. Khlopenkov, T. Kobuchi, A. Kostrioukov, R. Kumazawa, Y. Liang, S. Masuzaki, T. Minami, J. Miyazawa, T. Morisaki, S. Morita, H. Nakanishi, Y. Narushima, K. Nishimura, N. Noda, H. Nozato, S. Ohdachi, Y. Oka, M. Osakabe, T. Ozaki, B. J. Peterson, A. Sagara, T. Saida, K. Saito, S. Sakakibara, R. Sakamoto, M. Sasao, K. Sato, T. Seki, M. Shoji, H. Suzuki, N. Takeuchi, N. Tamura, K. Tanaka, K. Toi, T. Tokuzawa, Y. Torii, K. Tsumori, K. Y. Watanabe, Y. Xu, S. Yamamoto, T. Yamamoto, M. Yoshinuma, K. Itoh, T. Satow, S. Sudo, T. Uda, K. Yamazaki, K. Matsuoka, O. Motojima, Y. Hamada and M. Fujiwara

Transport Barrier Formation by Application of Localized ECH in the LHD
Oct. 2002 (EX/C4-5Rb)

NIFS-760 T. Hayashi, N. Mizuguchi, H. Miura, R. Kanno, N. Nakajima and M. Okamoto
Nonlinear MHD Simulations of Spherical Tokamak and Helical Plasmas
Oct. 2002 (TH/6-3)

NIFS-761 K. Yamazaki, S. Imagawa, T. Muroga, A. Sagara, S. Okamura
System Assessment of Helical Reactors in Comparison with Tokamaks
Oct. 2002 (FT/P1-20)

NIFS-762 S. Okamura, K. Matsuoka, S. Nishimura, M. Isobe, C. Suzuki, A. Shimizu, K. Ida, A. Fujisawa, S. Murakami, M. Yokoyama, K. Itoh, T. Hayashi, N. Nakajima, H. Sugama, M. Wakatani, Y. Nakamura, W. Anthony Cooper
Physics Design of Quasi-Axisymmetric Stellarator CHS-qa
Oct. 2002 (IC/P-07)

NIFS-763 Lj. Nikolic, M.M. Skoric, S. Ishiguro and T. Sato
On Stimulated Scattering of Laser Light in Inertial Fusion Energy Targets
Nov. 2002

NIFS-764
NIFS Contributions to 19th IAEA Fusion Energy Conference (Lyon, France, 14-19 October 2002)
Nov. 2002

NIFS-765 S. Goto and S. Kida
Enhanced Stretching of Material Lines by Antiparallel Vortex Pairs in Turbulence
Dec. 2002

NIFS-766 M. Okamoto, A.A. Maluckov, S. Satake, N. Nakajima and H. Sugama
Transport and Radial Electric Field in Torus Plasmas
Dec. 2002

NIFS-767 R. Kanno, N. Nakajima, M. Okamoto and T. Hayashi
Computational Study of Three Dimensional MHD Equilibrium with m/n=1/1 Island
Dec. 2002

NIFS-768 M. Yagi, S.-I. Itoh, M. Kawasaki, K. Itoh and A. Fukuyama
Multiple-Scale Turbulence and Bifurcaion
Jan. 2003

NIFS-769 S.-I. Itoh, K. Itoh and S. Toda
Statistical Theory of L-H Transition and its Implication to Threshold Database
Jan. 2003

NIFS-770 K. Itoh
Summary: Theory of Magnetic Confinement
Jan. 2003

NIFS-771 S.-I. Itoh, K. Itoh and S. Toda
Statistical Theory of L-H Transition in Tokamaks
Jan. 2003

NIFS-772 M. Stepic, L. Hadzievski and M.M. Skoric
Modulation Instability in Two-dimensional Nonlinear Schrodinger Lattice Models with Dispersion and Long-range Interactions
Jan. 2003

NIFS-773 M.Yu. Isaev, K.Y. Watanabe, M. Yokoyama and K. Yamazaki
The Effect of Hexapole and Vertical Fields on α-particle Confinement in Heliotron Configurations
Mar. 2003

NIFS-774 K. Itoh, S.-I. Itoh, F. Spineanu, M.O. Vlad and M. Kawasaki
On Transition in Plasma Turbulence with Multiple Scale Lengths
May 2003

NIFS-775 M. Vlad, F. Spineanu, K. Itoh, S.-I. Itoh
Intermittent and Global Transitions in Plasma Turbulence
July 2003

NIFS-776 Y. Kondoh, M. Kondo, K. Shimoda, T. Takahashi and K. Osuga
Innovative Direct Energy Conversion Systems from Fusion Output Thermal Power to the Electrical One with the Use of Electronic Adiabatic Processes of Electron Fluid in Solid Conductors.
July 2003

NIFS-777 S.-I. Itoh, K. Itoh and M. Yagi
A Novel Turbulence Trigger for Neoclassical Tearing Modes in Tokamaks
July 2003

NIFS-778 T. Utsumi, J. Koga, T. Yabe, Y. Ogata, E. Matsunaga, T. Aoki and M. Sekine
Basis Set Approach in the Constrained Interpolation Profile Method
July 2003